Nanoscale Res Lett (2009) 4:1389–1394
DOI 10.1007/s11671-009-9410-y

NANO EXPRESS

Photoelectric Properties of Silicon Nanocrystals/P3HT Bulk-Heterojunction Ordered in Titanium Dioxide Nanotube Arrays

Vladimir Švrček · Ivan Turkevych · Michio Kondo

Received: 24 June 2009 / Accepted: 5 August 2009 / Published online: 18 August 2009

Abstract A silicon nanocrystals (Si-ncs) conjugated-polymer-based bulk-heterojunction represents a promising approach for low-cost hybrid solar cells. In this contribution, the bulk-heterojunction is based on Si-ncs prepared by electrochemical etching and poly(3-hexylthiophene) (P3HT) polymer. Photoelectric properties in parallel and vertical device-like configuration were investigated. Electronic interaction between the polymer and surfactant-free Si-ncs is achieved. Temperature-dependent photoluminescence and transport properties were studied and the ratio between the photo- and dark-conductivity of 1.7 was achieved at ambient conditions. Furthermore the porous titanium dioxide (TiO_2) nanotubes' template was used for vertical order of photo-sensitive Si-ncs/P3HT-based blend. The anodization of titanium foil in ethylene glycol-based electrolyte containing fluoride ions and subsequent thermal annealing were used to prepare anatase TiO_2 nanotube arrays. The arrays with nanotube inner diameter of 90 and 50 nm were used for vertical ordering of the Si-ncs/P3HT bulk-heterojunction.

Keywords Silicon nanocrystals · Bulk heterojunction · Titanium dioxide nanotubes

Introduction

Most of the solar cells installed today are made of silicon. The vision is to produce solar cells from cheap materials in low-cost processes, thus resulting in lower cost electricity production. It is believed that bulk-heterojunction solar cells made of from conjugated polymer blends offer such a possibility [1, 2]. Organic semiconductors propose simple device fabrication technologies (i.e., screen printing and spin casting) at low temperature and therefore are very attractive for photovoltaic industry [3]. The bulk-heterojunction concept for solar cells has a potential to be considerably improved [2–4]. One possible route is the introduction of organic electron acceptors into a conjugated polymer matrix. Silicon in the form of tiny Si-ncs, which exhibit quantum confinement effects, offers unique properties: i.e., the Si-ncs can serve as electron acceptors [5, 6] and can produce multiple electrons per photon due to the carrier multiplication that can increase photocurrent generation [7]. The bulk-heterojunction based on Si-ncs can present new possibilities to design new types of absorber materials for low-cost hybrid solar cells [5–7].

The photovoltaic performance of Si-ncs/conductive polymer bulk-heterojunction relies on mesoscopic arrangement of both nanocrystals and polymer conjugation chains. The morphology of the bulk-heterojunction can be significantly affected by various fabrication parameters during the device formation [8]. Functional nanotubes fabrication and novel synthetic strategies for generating nanotubes from inorganic materials have been recently widely investigated and reported in literature [9]. An incorporation of novel 1D nanostructures into nano-porous templates and an enhancement of the solar cells performance based on 1D configurations have been recently demonstrated [10, 11]. It is expected that a fiber- and/or vertical 1D-like order of photosensitive bulk-heterojunction gives considerable advantages over the thin film technology, because it provides larger interfacial area for efficient exciton dissociation and straight path for photogenerated carries. Furthermore, fiber arrays have much

V. Švrček (✉) · I. Turkevych · M. Kondo
Research Center for Photovoltaics,
National Institute of Advanced Industrial Science
and Technology (AIST), Central 2, Umezono 1-1-1,
Tsukuba 305-8568, Japan
e-mail: vladimir.svrcek@aist.go.jp

lower reflectance and enable fabrication of thicker devices with increased absorption compared with thin films. As a result, fibers help to avoid circuit shorts and interruption of percolation paths for carriers to their respective electrodes [8]. Till date several nanotubular architectures have been investigated for potential enhancement of electron percolation pathways in bulk-heterojunction [8, 12]. One of such possibilities is vertically oriented titanium dioxide (TiO_2) nanotube arrays. An efficient charge collection in photoelectrochemical devices after blend infiltration into transparent TiO_2 nanotube films has been shown [13]. In addition, such architecture allows an improvement in light harvesting as thicker devices can be produced in order to increase the optical density [14]. A relatively easy fabrication technique of TiO_2 nanotube arrays by anodization offers highly ordered nano-templates at low cost [15, 16].

In this study, the bulk-heterojunction based on Si-ncs prepared by electrochemical etching and poly(3-hexylthiophene) (P3HT) polymer is investigated. Firstly, the phototransport properties of the bulk-heterojunction fabricated in parallel configuration on interdigitated electrodes are studied. Next, a vertical 1D-like configuration of the bulk-heterojunction through infiltration into a nanotubular template of anodic TiO_2 is performed. Anodization of titanium foil followed by annealing has been used to fabricate the crystalline anatase nanotubular templates. The optoelectrical properties of photoconductive Si-ncs/P3HT bulk-heterojunction aligned in TiO_2 nanotubes with inner diameter of 90 and 50 nm are compared and discussed in details.

Experimental Details

Firstly, in order to infiltrate the bulk-heterojunction, the TiO_2 nanotubes with two deferent inner diameters were prepared as follows. A 99.99% pure titanium foil was anodized in 0.3 wt% solution of NH_4F in ethylene glycol in a two-electrode configuration under constant potentials of 40 and 20 V at room temperature, respectively [15]. The titanium foil served as anode and platinum mesh as the counter electrode. The transformation of amorphous as-grown anodic TiO_2 into crystalline anatase was performed by annealing in air at 450 °C [16].

Secondly, following our previous work, the freestanding Si-ncs were prepared by electrochemical etching of silicon wafers [17]. Crystalline silicon boron-doped wafer with resistivity of 0.5–0.75 Ohm cm was used. The wafers were electrochemically etched in a mixture of hydrofluoric acid with pure ethanol and then the Si-ncs were harvested by mechanical scratching and sedimentation [5, 17]. After dispersion in ethanol, we could observe bright room temperature photoluminescence (PL) in the colloid solution by naked eye. The typical emission of Si-ncs used in this study is shown in Fig. 1a. The strong orange PL can be observed at room temperature under the excitation by a He:Cd CW laser (325 nm). After evaporation of the ethanol, the freestanding Si-ncs showed broad PL spectra with a maximum typically located around ~600 nm [18].

Then, the dried Si-ncs were used for bulk-heterojunction fabrication. Commercially available (ALDRICH, Nakayama, Tsukuba-branch, Japan) P3HT polymers were dissolved in chlorobenzene (14 mg/mL). An aliquot of 400 mg of the polymer solution and 2 mg of Si-ncs were mixed. The photoelectric properties of the blend were investigated in two configurations. For parallel photoconductivity measurements, the Si-ncs/P3HT blend was coated on interdigitated platinum contact evaporated on glass [5]. For perpendicular measurements, the Si-ncs/P3HT blend was incorporated into the TiO_2 nanotubes and covered on top by a transparent conductive oxide (TCO) electrode, which was spin-coated with poly(3,4-ethylenedioxythiophene) poly(styrenesulfonate) (PEDOT:PSS), to form TCO/PEDOT:PSS/(Si-ncs/P3HT)/TiO_2-NTs device. Another device with only pure P3HT polymer was prepared for comparison. All samples were dried at 140 °C for 30 min in vacuum.

The temperature-dependent PL measurements were run from 4 to 300 K by placing the samples into a cryostat. The He:Cd CW laser (325 nm or 3.82 eV) has been used as an excitation source. The conductivity and photo-conductivity measurements were performed in ambient conditions.

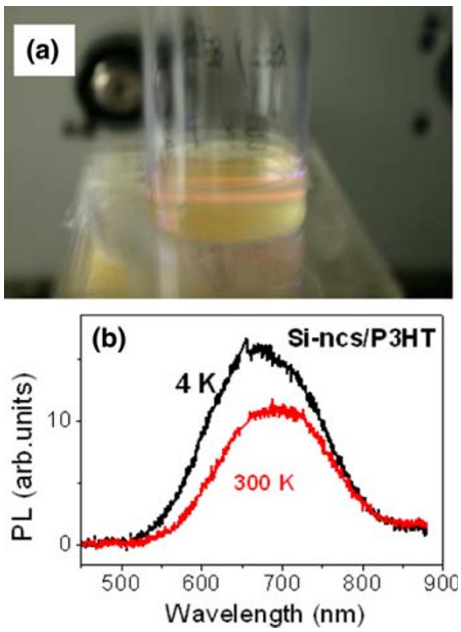

Fig. 1 **a** PL emission from Si-ncs dispersed in ethanol at room temperature and under the excitation by a He:Cd CW laser (325 nm). **b** PL spectra measured for Si-ncs/P3HT blend film under excitation at 325 nm taken at 4 and 300 K

A constant potential from a regulated dc power supply was applied and the resulting current was measured with an ampere meter (Sub-Femtoamp, Keithley 6430). For the photo-conductivity measurements, a white light of 1.5 AM was used to irradiate the samples.

Results and Discussions

Bulk-Heterojunction in Parallel Configuration

Figure 1b shows PL spectra measured for Si-ncs/P3HT blend film under excitation at 325 nm taken at 4 and 300 K. The introduction of the Si-ncs into the conjugated polymer results in change of the PL characteristics [18]. Contrary to the pure polymer films, the red shift of the PL band as a function of temperature is recorded. A similar temperature dependence of the PL behavior was previously observed for Si-ncs with quantum confinement size effect, which was introduced into MEH-PPV polymer [18]. After exciton transfer from the polymer to the Si-ncs, the state filling effect is responsible for the shift of the PL band [19]. An increase in temperature decreases the emission intensity at higher emission energies and leads to a ~40-nm red-shift of PL spectrum maxima in temperature ranging from 4 to 300 K (Fig. 1b).

The parallel photo-conductivity is applied to check the bulk-heterojunction formation [5]. Figure 2a represents a schematic sketch of the experimental setup when the Si-ncs/P3HT bulk-heterojunction is spin-coated on interdigitated electrodes. It is believed that placing of both negative and positive contacts on the backside of the solar cell eliminates the front contact and provides a potential to improve short-circuit current [5]. Furthermore, this configuration could lead to an easier interconnection and a simpler way to module fabrication [20]. In our particular case, the introduction of the Si-ncs into the polymer increases the porosity of the blend and we can eliminate shunting of Si-ncs/P3HT bulk-heterojunction when we spin-coat a large surface area [5].

Figure 2b displays the current–voltage (*I–V*) curves for Si-ncs/P3HT blend in dark (black line) and under AM1.5 illumination (red line). An introduction of the Si-ncs into P3HT polymer increases the overall dark-conductivity (more than two times) through the polymer. Furthermore, under AM1.5 illumination, the photocurrent generation is observed. The ratio of the photo-conductivity to the dark-conductivity is about 1.7. We attribute the photocurrent generation to the formation of the bulk-heterojunction in the Si-ncs/P3HT blend. To form the bulk-heterojunction, the photosensitive material requires proper energy band alignment. Fortunately, the energy levels of Si-ncs match the energy levels of the conjugated P3HT polymer. The highest

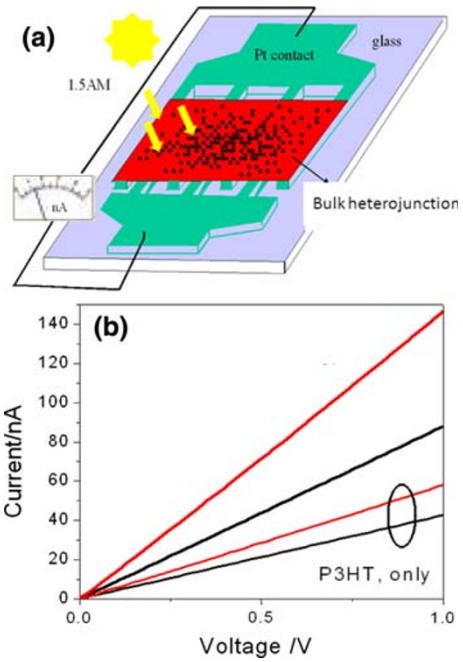

Fig. 2 **a** Schematic representation of the Si-ncs/P3HT bulk-heterojunction spin coated on interdigitated electrodes. **b** *I–V* curves for Si-ncs/P3HT blend. The *I–V* characteristics of P3HT polymer are only shown for comparison. *Black lines* represent the measurement in *dark and red lines* under AM1.5 illumination

occupied molecular orbital for P3HT is −5 eV below the vacuum, whereas the lowest unoccupied molecular orbital is −3 eV. The band gap of Si-ncs is about (~2 eV) [5], which allows a proper adjustment of the bands for the *e–h* separation [5]. The different electron affinities and ionization potentials provide a driving force for the *e–h* dissociation when the excitons are generated under AM1.5 irradiation. We assume that a large fraction of the excitons dissociates at Si-ncs/polymer interface. Dissociated excitons leave the electrons in the nanocrystals and the holes in the polymer.

Alignment of Bulk-Heterojunction in TiO_2 Nanotubes

The morphology of the TiO_2 nanotube layer after thermal treatment is summarized in Fig. 3. Figure 3a, b shows scanning electron microscopy (SEM) images of TiO_2 nanotubes with average diameters of 50 and 90 nm, respectively, and with lengths of about 1 μm. In both cases, the transformation of amorphous TiO_2 into crystalline anatase was confirmed by XRD measurements. Figure 3c shows typical XRD spectra after the annealing process. Two most important TiO_2 anatase peaks corresponding to (101) and (200) orientations were clearly recorded.

It is observed that infiltration of photosensitive Si-ncs/P3HT blend in the TiO_2 nanotubes results in increase in the photovoltage generation. The corresponding *I–V*

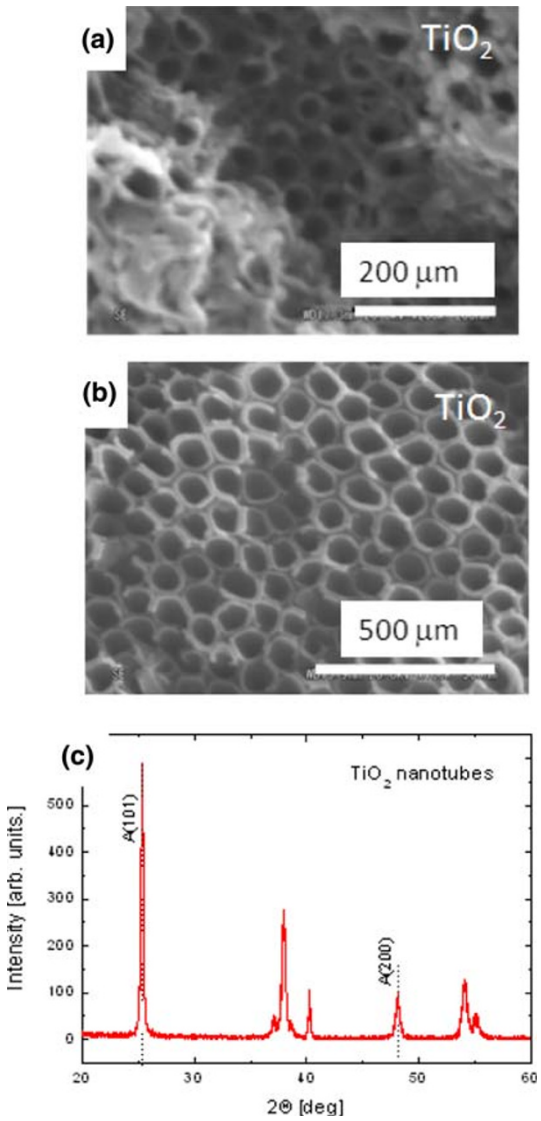

Fig. 3 **a** SEM image of the nanotubular TiO_2 template used for vertical order of Si-ncs/P3HT bulk-heterojunction. **b** XRD spectra that reveals transformation of as-grown amorphous TiO_2 nanotubes into a single phase anatase after annealing at 450 °C

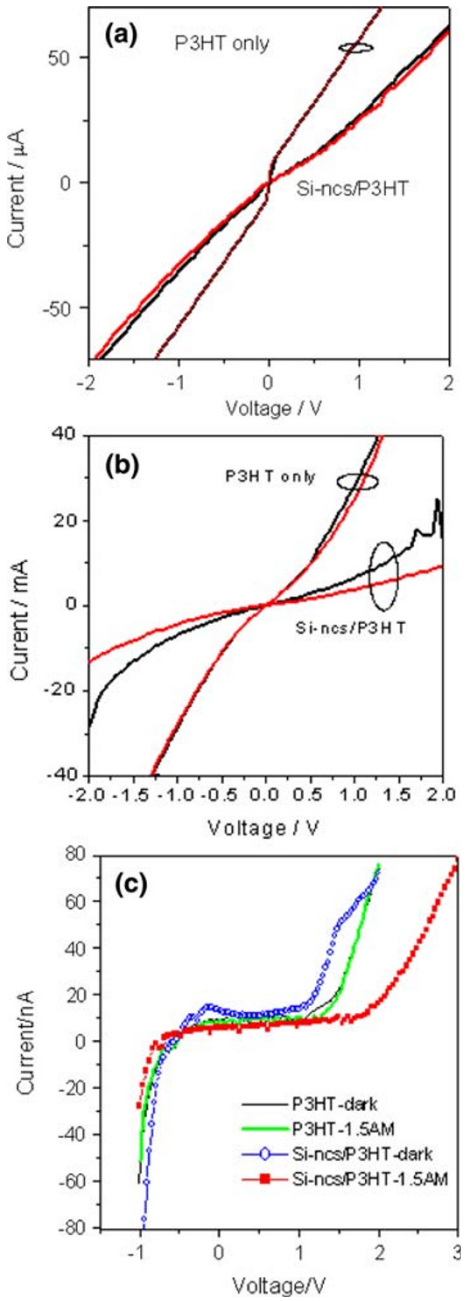

Fig. 4 *I–V* characteristics of the sandwiched Si-ncs/P3HT bulk-heterojunction in the dark and under illumination at AM1.5 after annealing at 140 °C. The *I–V* characteristics were taken from the blend sandwiched on solid nonporous substrate (**a**) and within TiO_2 nanotube arrays with the diameters of 50 nm (**b**) and 90 nm (**c**), respectively. The *I–V* characteristics of pure polymer are shown for comparison

characteristics of Si-ncs/P3HT heterojunction in vertical configuration in the dark and under illumination at AM1.5 after annealing at 140 °C are compared in Fig. 4. The *I–V* characteristics of the blend sandwiched on solid nonporous substrate are presented in Fig. 4a. Similar to the parallel configuration (Fig. 3b), the introduction of Si-ncs in P3HT polymer increases *I–V* curve bending and the photo-conductivity response. Both features are further enhanced when the bulk-heterojunction is introduced into the TiO_2 nanotubes. Figure 4b, c represents the *I–V* characteristics of the blends infiltrated into TiO_2 nanotubes with diameters of 50 and 90 nm, respectively. The *I–V* characteristics for both the pure polymer and bulk-heterojunction show a *p–i–n* behavior. However, superior open voltage and ratio between the photo- and dark-conductivity are observed in the case of infiltration of the blend into nanotubes with larger diameter (Fig. 4c, red line).

One can expected that the alignment of Si-ncs/P3HT bulk-heterojunction within TiO_2 nanotubes, which are perpendicular to the contact, will facilitates charge transfer

along the nanotubes [21]. Figure 5 displays a schematic sketch of the structure used in this study. At the same time, the alignment within the nanotubes can reduce losses incurred by charge hopping across the Si-ncs/P3HT blend. The typical range of exciton diffusion lengths in polymers is 5–20 nm. Therefore, one can expect that the nanotube size should be around this range in order to promote an efficient charge separation. However, the polymer chain packing inside small nanotubes can be fundamentally different from the chain packing in a bulk film [12]. In the bulk film, the high degree of π–π stacking between the polymer chains allows the delocalization of excitons over multiple chains. This can be eliminated in the case of confinement of the polymer in nanotubes. Similar to our architecture, it has been found [22] that the mobility of P3HT polymer infiltrated into an anodic alumina template with vertical channels was enhanced by as much as a factor of 20 due to alignment of the polymer chains in the pores in a direction perpendicular to the substrate. However, other group pointed out [23] that in small pores, the chains of the conjugated polymer were found to be isolated with little evidence of interchain contact. Similar to those reported effects, one could expect that infiltration of Si-ncs/P3HT polymer-based bulk-heterojunction into TiO_2 nanotubes will result in alignment of the polymer chains. However, further studies should be performed in order to find an optimum diameter of nanotubes for a proper alignment of polymer, which contains Si-ncs.

The photovoltage generation in the bulk-heterojunction most likely results in increase in open circuit voltage. However, the voltage open-circuit values cannot be explained by the metal–insulator–metal model [24]. In this case, the polymer blend has a negligible amount of intrinsic charge carriers and is considered as an insulator. The upper limit of the open-circuit voltage can be estimated from the difference of the two electrodes work functions. Figure 6 shows corresponding energy level diagram of the blend

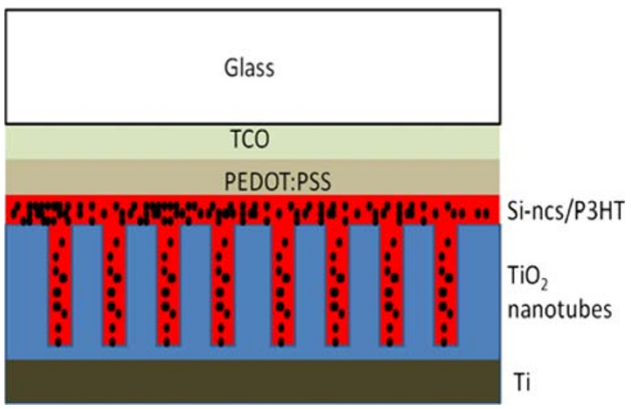

Fig. 5 Schematic sketch of the structure for ordering of Si-ncs/P3HT bulk-heterojunction in TiO_2 nanotube arrays

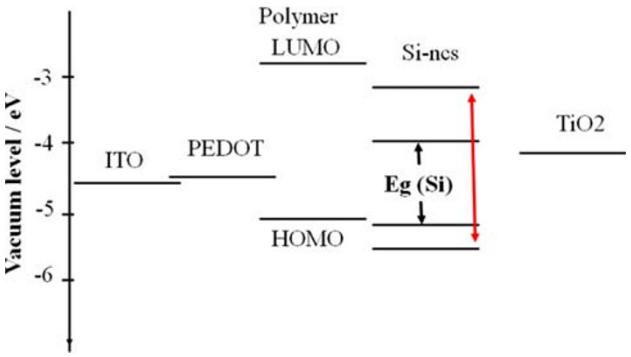

Fig. 6 Energy level diagram of Si-ncs conjugated P3HT polymer blends sandwiched between TCO and TiO_2 nanotube arrays

sandwiched between PEDOT:PSS contact and TiO_2 nanotubular template. On the other hand, small difference of the electrodes work functions results in a weak photocurrent generation. Even more, the presence of the Si-ncs in polymer makes the blend to be more semiconductor rather than an insulator; therefore, a high-voltage open-circuit can be partially explained by assuming a Schottky barrier at the Si-ncs/P3HT/PEDOT:PSS interface.

It is clear that the nanofiber morphology of the blend embedded into nanotubular templates can contribute to high open-circuit voltage as well. The bulk-heterojunction performance depends on mesoscopic arrangement of both nanocrystals and polymer chains. The fiber-like alignment provides larger interfacial area, which results in enhanced exciton dissociation. It has to be noted that compared to thin films, the fiber arrays configuration has lower reflectance. This is also most likely the reason in the case of TiO_2 nanotubes with larger diameter that allow infiltration of larger amount of bulk-heterojunction into nanotubes, and form thicker device. As a result, increased absorption and active surface area for exciton separation augment photovoltage generation. However, for a clear picture of the origin of an increase in the open-circuit voltage, further experiments have to be performed.

Summary

We have investigated photoelectric properties of the Si-ncs P3HT polymer-based bulk-heterojunction. The room temperature luminescent Si-ncs with large optical band gap ($\sim$2 eV) were prepared by electrochemical etching. The presence of the Si-ncs in the polymer increases the transport and assures an interaction between electronic states of the Si-ncs and P3HT polymer. As a result, the exciton transfer from the polymer and bulk-heterojunction formation were achieved. The exciton transfer and quantum confinement effect in Si-ncs lead to PL maxima shift

around ~40 meV in the temperature region 4–300 K. The ratio between photo- and dark-conductivity around 1.7 in parallel configuration has been demonstrated. Furthermore, we showed that the titanium dioxide (TiO_2) nanotube arrays with tunable nanotube diameter can be efficient for a vertical 1D-like order of Si-ncs/P3HT photosensitive blend. The arrangement of the Si-ncs/P3HT bulk-heterojunction within ordered TiO_2 nanotubes prepared perpendicular to the contact facilitates excitons separation and charge transfer along nanotubes. It is expected that the optimization of the morphology of the Si-ncs/P3HT blend infiltrated into TiO_2 nanotubes can lead to an improvement in the solar cell performance.

Acknowledgment This study was supported by the New Energy Development Organization (NEDO) of Japan.

References

1. G. Yu, A.J. Heeger, Charge separation and photovoltaic conversion in polymer composites with internal donor/acceptor heterojunctions. J. Appl. Phys. **78**, 4510 (1995)
2. J.J.M. Halls, C.A. Walsh, N.C. Greenham, E.A. Marseglia, R.H. Friend, S.C. Moratti, A.B. Holmes, Efficient photodiodes from interpenetrating polymer networks. Nature **376**, 498 (1995)
3. S.E. Shabeen, D.S. Ginley, G.E. Jabbour, Organic-based photovoltaics: toward low-cost power generation. MRS Bull. **30**, 10 (2005)
4. G. Yu, J. Gao, J.C. Hummelen, F. Wudl, A.J. Heeger, Polymer photovoltaic cells: enhanced efficiencies via a network of internal donor–acceptor heterojunctions. Science **270**, 1789 (1995)
5. V. Švrček, H. Fujiwara, M. Kondo, Improved transport and photo-stability of poly[methoxy-ethylexyloxy-phenylenevinilene] polymer thin films by boron doped freestanding silicon nanocrystals. Appl. Phys. Lett. **92**, 143301 (2008)
6. C. Lui, Z. Holman, U. Kortshagen, Hybrid solar cells from P3HT and silicon nanocrystals. Nano Lett. **9**, 449 (2009)
7. M.C. Beard, K.K. Knutsen, P. Yu, J. Luther, Q. Song, R.J. Ellingson, A.J. Nozik, Multiple exciton generation in colloidal silicon nanocrystals. Nano Lett. **7**, 2506 (2007)
8. S.S. Williams, M.J. Hampton, V. Gowrishankar, I.-K. Ding, J.L. Templeton, E.T. Samulski, J.M. DeSimone, M.D. McGehee, Nanostructured titania-polymer photovoltaic devices made using PFPE-based nanomolding techniques. Chem. Mater. **20**, 5229 (2008)
9. C. Yan, J. Liu, F. Liu, J. Wu, K. Gao, D. Xue, Tube formation in nanoscale materials. Nanoscale Res. Lett. **3**, 473 (2008)
10. Z. Wang, M. Brust, Fabrication of nanostructure via self-assembly of nanowires within the AAO template. Nanoscale Res. Lett. **2**, 34 (2007)
11. K. Yu, J. Chen, Enhancing solar cell efficiencies through 1-D nanostructures. Nanoscale Res. Lett. **4**, 1 (2009)
12. K.M. Coakley, Y.X. Liu, M.D. McGehee, K.L. Frindell, G.D. Stucky, Infiltrating semiconducting polymers into self-assembled mesoporous titania films for photovoltaic applications. Adv. Funct. Mater. **13**, 301 (2003)
13. G.K. Mor, K. Shankar, M. Paulose, O.K. Varghese, C.A. Grimes, High efficiency double heterojunction polymer photovoltaic cells using highly ordered TiO_2 nanotube arrays. Appl. Phys. Lett. **91**, 152111 (2007)
14. M. Law, L.E. Greene, J.C. Johnson, R. Saykally, P.D. Yang, Nanowire dye-sensitized solar cells. Nat. Mater. **4**, 455 (2005)
15. H.E. Prakasam, K. Shankar, M. Paulose, O.K. Varghese, C.A. Grimes, A new benchmark for TiO_2 nanotube array growth by anodization. J. Phys. Chem. C **111**, 7235 (2007)
16. J.M. Macak, S. Aldabergerova, A. Ghicov, P. Schmuki, Smooth anodic TiO_2 nanotubes: annealing and structure. Phys. Status Solidi A **203**, R67 (2006)
17. V. Švrček, A. Slaoui, J.-C. Muller, Ex-situ prepared Si nanocrystals: their elaboration and characterization in embedded silica glass. J. Appl. Phys. **95**, 3158 (2004)
18. V. Švrcek, H. Fujiwara, M. Kondo, Luminescent properties of doped freestanding silicon nanocrystals embedded in MEH-PPV. Sol. Energy Mater. Sol. Cells **93**, 774 (2009)
19. M.L. Brongersma, A. Polman, K.S. Min, E. Boer, T. Tambo, H.A. Atwater, Tuning the emission wavelength of Si nanocrystals in SiO_2 by oxidation. Appl. Phys. Lett. **72**, 2577 (1998)
20. K. Nakamura, T. Isaka, Y. Funakoshi, Y. Tonomura, T. Machida, K. Okamoto, 20th European Photovoltaic Solar Energy Conference, Barcelona (2005)
21. R. Tenne, C.N.R. Rao, Inorganic nanotubes. Philos. Trans. R. Soc. A **362**, 2099 (2004)
22. K.M. Coakley, B.S. Srinivasan, J.M. Ziebarth, C. Goh, Y. Liu, M.D. McGehee, Enhanced hole mobility in regioregular polythiophene infiltrated in straight nanopores. Adv. Funct. Mater. **15**, 1927 (2005)
23. A.J. Cadby, S.H. Tolbert, Controlling optical properties and interchain interactions in semiconducting polymers by encapsulation in periodic nanoporous silicas with different pore sizes. J. Phys. Chem. B **109**, 17879 (2005)
24. I.D. Parker, Carrier tunneling and device characteristics in polymer light-emitting diodes. J. Appl. Phys. **75**, 1656 (1994)